

Debris-flow behavior containing fine sediment considering phase shift

Kana Nakatani^{a,*}, Yuji Hasegawa^b, Yusuke Asano^a, Yoshifumi Satofuka^c

^a Graduate School of Agriculture, Kyoto University, Oiwake-cho, Kitashirakawa, Sakyo-ku, Kyoto 6068502, Japan

^b Graduate School of Integrated Arts and Sciences, Hiroshima University, 1-7-1 Kagamiyama, Higashi Hiroshima, Hiroshima 7398251, Japan

^c Department of Civil Engineering, Ritsumeikan University, 1-1-1 Noji-higashi, Kusatsu, Shiga 5258577, Japan

Abstract

Recent observations have shown that debris flows containing fine particles in volcanic regions exhibit greater mobility compared to stony debris flows. Recent researches have described that greater mobility occurred from fine sediment phase shift from solid phase to fluid phase in debris flow. In Japan, debris-flow research and sabo or erosion control planning widely apply the equilibrium concentration methods proposed by Takahashi. For considering fine sediment phase shift with the equilibrium method, it is proposed to set high fluid density. However, the mechanism of phase shift and behaviours of debris flows with fine sediment, are not fully understood. In this study, we conducted hydraulic experiments with sediment particles of two different diameters, defined as fine sediment and coarse sediment. We applied the equilibrium methods and took into account the increased fluid phase density due to the sediment phase shift to fluid. From the results, we found that part of the fine particles contribute to the increase in the fluid phase density. When conducting experiments, not only fine sediment, but some parts of coarse sediment behaved as a fluid. For considering the shift of sediment to fluid phase in debris flows, we presumed that the flow turbulence in debris flow affected. Regarding the sediment concentration, higher total sediment (coarse and fine) concentration increased the fluid phase density. A larger ratio of coarse sediment increased the fluid phase density more than when sediment contained only fine particles. It was speculated to occur from the flow turbulence owing to the mixture condition. Cases with smaller total sediment discharge showed higher fluid phase density though in same sediment concentration. We also found that the larger dimensionless tractive force showed a smaller ratio behaving as fluid phase, which was in contrast with the trends in recent studies.

Keywords: debris flow, fine sediment, phase shift, laboratory experiment

1. Introduction

Debris flows occur due to various phenomena including landslides, river bed erosion, and landslide dam outbursts (e.g., Iverson, 1997; Takahashi, 1991). Damage from debris flows is serious due to their high mobility. In Japan, many debris flows occurred in Hiroshima Prefecture in 2014 and in 2018 (Kaibori et al., 2018). Reports show that the sediment particle distribution in these debris flows was wide ranging from fine particles to large boulders, as shown in Fig.1. There are many studies on debris flows but most of them are focused on the stony debris flows with large sediment particles, in particular, on the concentration of coarser particles in the front of the flow (e.g., Wada et al., 2015). In Aso (Kumamoto Prefecture, Japan), debris flows containing high concentrations of fine particles occurred in 2012. They showed high mobility, and the sediment deposition extended outside of the debris-flow-risk designated areas, reaching to mild-slope areas with slopes less than 2 degrees (Ministry of Land, Infrastructure, Transport and Tourism, 2014). These debris-flow characteristics are different from what is typical for stony debris flows.

In Japan, the equilibrium concentration equation (Takahashi, 1991) appears widely in studies on debris flows and on countermeasure planning using sabo (sedimentation and erosion control) works. To be applicable to debris flows containing fine sediments, the methods should consider the change of phase by fine sediment to fluid phase (e.g. Uchida et al., 2013). It is confirmed that setting higher fluid density in the method described higher mobility of debris

* Corresponding author e-mail address: kana2151@kais.kyoto-u.ac.jp

flows containing fine sediment. Some studies have proposed that fine sediment should be taken into interstitial fluid turbulence to cause phase shift by fine sediment to fluid phase (e.g. Nishiguchi et al., 2011; Hotta and Miyamoto, 2008). Furthermore, some experiment results showed not only fine sediments, but part of the coarse sediment, behaved as a fluid (Nakatani et al., 2018). However, the mechanism and behaviors of debris flows with fine sediments, and also the method needed to estimate the proper fluid density, are not clear.

In this study, we focused on debris flows composed of sediment particles with two different diameters: defined as fine sediment and coarse sediment, and conducted hydraulic experiments. We also considered the effect of the sediment concentration, the mixing ratio of different sized particles, the hydraulic conditions, and the turbulence intensity on debris-flow behavior and fluid phase density.



Fig. 1. Debris flow that occurred in the 2014 Hiroshima sediment disaster

2. Methods

2.1. Laboratory experiment methods

The experimental setup is shown in Fig. 2a. The experimental channel is a rectangular straight open channel 5-m long and 10-cm wide with a variable slope. In this study, we set the flume angle for each cases not to cause larger gap than 3 degrees from equilibrium state slope angle. We supplied constant water from the upstream tank. For the sediment supply, we used two hoppers. The first hopper supplied fine sediment and was positioned set 450 cm upstream from the downstream end. The second hopper supplied coarse sediment and was positioned set 400 cm upstream from the downstream end. We set fine sediment hopper at upstream side because smaller particle requires more time and space to mix with water comparing to larger particle.

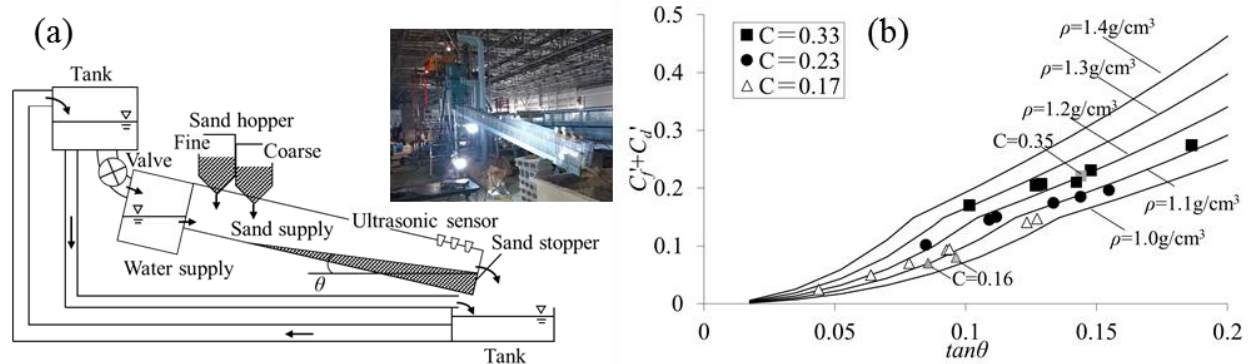


Fig.2. (a) Experimental flume setup and (b) results showing the relationship between slope and solid phase sediment concentrations (legend C describes the supplied total sediment concentration)

We used two types of uniform sediment particles: 0.13 mm as fine sediment and 2.81 mm as coarse-grained sediment. The sediment density σ was 2.61 g/cm^3 , and internal friction angle of the sediment ϕ was 35 deg. We conducted 23 cases, as shown in Table 1 (left 5 elements showing experiment conditions). We placed a high-speed camera (Ex-F1, Casio, Japan) with 300 fps at 50 cm upstream from the downstream end of the flume. We measured the flow depth from video because ultrasonic sensor could not distinguish riverbed deposition. We defined riverbed where soil particles did not move. In Case 16, the condition was rather unstable compared to other cases, and we could not determine a flow depth.

Table 1. Experiment conditions and results

Case	Experiment conditions (5 elements)					Results (5 elements)				
	Supplied water	Supplied sediment (fine)	Supplied sediment (coarse)	Sediment concentration	Ratio of fine and coarse sediment	Deposit slope θ	Flow depth h	Ratio of fine sediment behave as fluid phase	Ratio of coarse sediment behave as fluid phase	Fluid phase density ρ
	cm ³ /s	cm ³ /s	cm ³ /s	$C_f + C_d$	$C_f : C_d$	deg.	cm	C_f'' / C_f	C_d'' / C_d	g/cm ³
1	1500	370	370	0.33	1:1	10.56	1.6	0.34	0	1.12
2	1500	150	150	0.17	1:1	7.03	2.2	0.35	0	1.05
3	1500	150	300	0.23	1:2	8.19	1.4	0.58	0	1.09
4	1000	300	0	0.23	3:0	8.80	2.0	0.15	(only C_f)	1.07
5	1000	165	330	0.33	1:2	7.22	1.6	1.00	0.07	1.25
6	1000	250	250	0.33	1:1	7.28	1.3	0.75	0	1.25
7	1000	100	200	0.23	1:2	6.23	1.3	1.00	0.05	1.16
8	1000	150	150	0.23	1:1	7.61	1.6	0.49	0	1.11
9	1000	70	140	0.17	1:2	4.48	1.3	1.00	0.36	1.17
10	1000	100	100	0.17	1:1	5.30	1.3	0.93	0	1.14
11	1000	90	120	0.17	3:4	5.36	1.3	1.00	0.01	1.13
12	600	100	200	0.33	1:2	7.35	1.0	1.00	0.05	1.25
13	600	150	150	0.33	1:1	5.79	0.9	0.96	0	1.31
14	600	90	90	0.23	1:1	6.38	0.8	0.69	0	1.15
15	600	60	60	0.17	1:1	2.50	1.0	1.00	0.75	1.24
16	600	300	0	0.33	3:0	8.41	-	0.30	(only C_f)	1.21
17	600	40	80	0.17	1:2	7.25	1.35	0.42	0	1.04
18	600	70	110	0.23	7:11	4.85	1.45	1.00	0.28	1.23
19	600	50	70	0.17	5:7	3.65	1.1	1.00	0.53	1.20
20	555	200	100	0.35	2:1	8.2	1.2	0.56	0	1.27
21	600	200	100	0.33	2:1	8.1	1.1	0.55	0	1.25
22	1550	200	100	0.16	2:1	4.9	3.5	0.87	0	1.16
23	1550	100	200	0.16	1:2	5.5	3.5	1.00	0.21	1.13

(- is showing the case flow depth could not measure)

At 15 cm, 30 cm, and 45 cm upstream from the downstream end of the flume, we set three ultrasonic sensors (from upstream, we called as No.1-No.3) with 50 Hz resolution (E4SC-DS30, Omron, Japan) and measured the flow surface slope from the flow surface height. At the downstream end, we installed 10 cm height sand stopper to cause deposition. For the initial condition, we set the sediment deposition as horizontal state for 10 cm height at downstream end to provide a movable bed condition. We supplied water and sediment for approximately 120 seconds, which was sufficient time for the deposit slope angle became stable.

We assumed equilibrium flow conditions were achieved when ultrasonic sensors showed the same value for 10 seconds. Each sensor measurement of the flow surface height and slope was calculated as the average value from three sensors. Using average slope from sensor No.1-No.2 and No.2-No.3, we also checked there was not significant difference with No.1-3. Here, we used the flow surface slope angle θ as river bed slope angle assuming that in the equilibrium state, the river bed slope and surface flow slope expected to become equal. Applying the supplied sediment concentration and the results of slope angle, we calculated fluid phase density using the equilibrium concentration method described in the next section.

2.2. Methods for estimating the fluid phase density

Different phases of debris flow are shown in Fig. 3. Fig.3a shows no phase shift conditions, so all the sediments behave as solid phase. Fig.3b shows that part of the fine sediment behaves as fluid phase, as reported in recent studies (e.g., Uchida et al., 2013). Fig.3c shows the fine sediment and part of the coarse sediment also behaving as fluid phase. Equation (1) shows the total sediment concentration C containing coarse sediment and fine sediment. Equation (2) shows the constitution of fine sediment considering different phases.

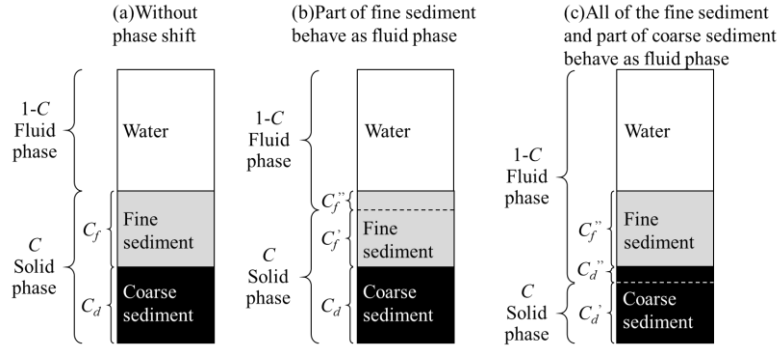


Fig. 3. Images of phases in debris flow (a) no phase shift, (b) part of fine sediment behaves as fluid phase, (c) all the fine sediment and part of the coarse sediment behaves as fluid phase.

$$C = C_d + C_f \quad (1)$$

$$C_f = C_f' + C_f'' \quad (2)$$

where C_d is the coarse sediment concentration, C_f is the fine sediment concentration, C_f' is the fine sediment concentration that behaves as solid phase, and C_f'' is the fine sediment concentration that behaves as fluid phase.

As in recent studies and in Fig. 3b, when considering fine sediment in debris flows behaving as solid and fluid phases, the following equation describes the fluid phase density ρ considering phase shift:

$$\rho = \frac{(1-C)\rho_w + C_f'' \cdot \sigma}{(1-C) + C_f''} \quad (3)$$

where σ is the mass density of the sediment and ρ_w is the mass density of pure water.

When applying the sediment concentration and the slope from our experiments, we can calculate the fluid phase density ρ using the equilibrium concentration method (Takahashi, 1991) for debris flow (equation 4) and for sediment sheet flow (equation 5). Applying equation (4) or equation (5) depends on the flow characteristics, especially on the degree of slope.

$$C_\infty = \frac{\rho \tan \theta}{(\sigma - \rho)(\tan \phi - \tan \theta)} \quad (\theta_x \leq \theta) \quad (4)$$

$$C_\infty = 6.7 \left\{ \frac{\rho \tan \theta}{(\sigma - \rho)(\tan \phi - \tan \theta)} \right\}^2 \quad (1.8 \leq \theta \leq \theta_x) \quad (5)$$

where C_∞ is the equilibrium concentration, θ is the slope angle, and ϕ is internal friction angle of the sediment.

When calculating the equilibrium concentration, we changed the fine sediment concentration behaving as fluid phase C_f'' , also changing the fluid phase density ρ , and repeated the calculation until the values of both equations for (3) and (4), or (3) and (5) became equal. After achieving equal values, we defined the fluid phase density ρ considering the fine sediment phase shift. And we also defined the solid phase sediment concentration excluding the concentration of the fine sediment behaving as fluid phase C_f'' .

We used the flow surface slope angle θ assuming that in the equilibrium state, the river bed slope and surface flow slope expected to become equal. Here, θ_x is the angle transition from debris flow to sediment sheet flow: $\rho = 1.0$

g/cm^3 and $\theta_x = 7.81$ deg. In the original equilibrium concentration, it is known that a discontinuous boundary occurs between debris flow (equation 4) and sediment sheet flow (equation 5) when the value of ρ changes from 1.0 g/cm^3 . Therefore, we applied this method to set the continuous boundary, changing θ_x as proposed in recent studies (e.g., Suzuki et al., 2013).

When the calculated fluid density ρ became larger than the condition under which all the fine sediment behaved as fluid phase, we assumed that part of the coarse sediment also behaved as fluid phase, as shown in Fig. 2c. In that case, the coarse sediment concentration C_d is as defined in equation (6) and the solid phase sediment C_{solid} is as defined in equation (7), as follows

$$C_d = C_d' + C_d'' \quad (6)$$

$$C_{solid} = C_d' + C_f' \quad (7)$$

where C_d' is the coarse sediment concentration that behaves as solid phase, and C_d'' is the coarse sediment concentration of that which behaves as fluid phase. In Fig. 2c, the right argument of equation (7) C_f' will be zero.

2.3. Experimental conditions

In Table 1, the left 5 elements show the experimental conditions and the right 5 elements show the experiment results. From Case 1–19, we set the supplied sediment concentration ($C_f + C_d$) as 0.33, 0.23, or 0.17, and changed the water supplied to $1500 \text{ cm}^3/\text{s}$, $1000 \text{ cm}^3/\text{s}$, or $600 \text{ cm}^3/\text{s}$. We also changed the ratio of fine sediment and coarse sediment (f:c), focusing in particular, on 1:1 and 1:2. In Case 20–23, we set the total supplied sediment to $300 \text{ cm}^3/\text{s}$, and changed the sediment concentration and particle size supply ratio.

3. Results And Discussion

In Fig. 2b, the graph shows the slope on the horizontal axis acquired from the result, and the calculated sediment concentration behaving as solid phase ($C_f' + C_d'$) on the vertical axis. The plots shown in the legend describe the total supplied sediment concentration ($C_f + C_d$). In the figure, the equilibrium concentration equations are also described, showing the change in the fluid phase density ρ from 1.0 g/cm^3 to 1.4 g/cm^3 .

From the results, all cases showed higher sediment concentration than expected with equilibrium concentration equations with fluid phase density $\rho = 1.0 \text{ g/cm}^3$. When the supplied sediment concentration was small, the fluid phase density ρ became small. When the supplied sediment concentration was constant, and the slope $\tan\theta$ was small, the fluid phase density ρ became large. From Table 1 (right 5 elements showing results) and Fig. 2b results, the supplied sediment concentration, and also the ratio of fine to coarse sediments suggested to affect the fluid phase density. This shows that the presence of coarse sediment influences the phase shift.

3.1. Factors affecting phase shift

Fig. 4 shows the experimental results for the debris flow phases: the upper part shows the effect of discharge and the lower part shows the effect of the particles and water ratio. Only the cases in which the supplied sediment ratio (fine to coarse: f:c) was (1:1) or (1:2) are described. The bar charts distinguished with a dotted line shows cases with the same supplied sediment concentration and the supplied sediment ratio f:c. For Case 23, the supplied concentration was 0.16, but it was placed with cases in which the concentration was 0.17.

All cases showed a phase shift to fluid phase for the fine sediment. In cases 5, 7, 9, 11, 12, 15, 18, 19, and 23, not only all the fine sediment, but also part of the coarse sediment was presumed to behave as fluid phase. In Case 15 and 19, more than half of the coarse sediment was presumed to behave as fluid phase. The supplied sediment concentration C was 0.17, the supplied sediment discharge was the smallest ($120 \text{ cm}^3/\text{s}$), and the ratio of fine to coarse sediment (f:c) was (1:1) and (5:7), respectively. However, when the supplied sediment concentration was $C = 0.17$, the supplied sediment discharge was $120 \text{ cm}^3/\text{s}$, and the ratio of fine to coarse sediment was (1:2); Case 17 did not show coarse sediment behavior as fluid phase. In the cases which coarse sediment behaving as fluid phase, the proportion of the coarse sediment was larger than that of the fine sediment, except for Case 15. Therefore, it is suggested that the mixture ratio of fine and coarse sediment affect the phase shift. On the other hand, the fluid phase density ρ became larger

than 1.25 g/cm^3 when the supplied sediment concentration was $C = 0.33$ (in Cases 5, 6, 12, and 13). Thus, the supplied sediment concentration and supplied sediment discharge indicated to affect the phase shift.

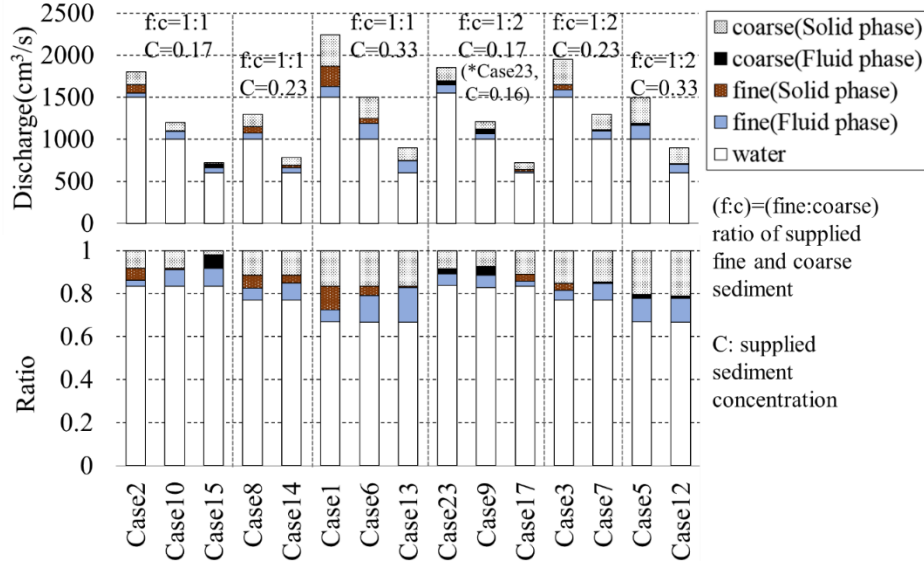


Fig. 4. Experimental results when the sediment supply fine-to-coarse ratio (in graph, shown as f:c) was 1:1 or 1:2

At the same sediment concentration, the space around sediment particles in debris flow becomes small when the sediment discharge is small. Generally, turbulence in debris flow occurs more easily when the space around sediment particles is large. And it is presumed that turbulence causes sediment phase shift from solid to fluid more easily (e.g. Nakatani et al., 2018). However, in our experiment, some case results showed a different trend. When the supplied fine-sediment discharge was large, the space around fine sediment particle became large, but showed lower fluid phase density indicating that there was difficulty completing the phase shift. This trend was especially clear in cases with the fine to coarse particle ratio of 1:1 (e.g., when the supplied sediment concentration C was 0.33: cases 1, 6, and 13).

When assuming that the space size around sediment particles in debris flow had become larger than the turbulence intensity influence range, we could explain the phenomenon that cases with large supplied fine sediment discharge resulted in lower fluid phase density indicating difficulty causing the phase shift. However, the cases in which the supplied sediment concentration $C = 0.33$ and the ratio of fine to coarse sediment was 1:2 (cases 5 and 12) showed almost the same fluid phase density, even though the supplied sediment discharge became large. In cases 5 and 12, it is suggested that the space size around sediment became close to the upper limit of the turbulence intensity influence range. On the other hand, when $C = 0.17$ and the ratio of fine to coarse sediment was 1:2 (cases 9 and 17), when the supplied sediment discharge was large, higher fluid phase density occurred which matches to the general approach. Here, it is presumed that the influence range of turbulence intensity influence was related to the amount of space around the sediment particles in debris flow, which can be considered from the supplied sediment discharge.

3.2. Considering the phase shift from turbulence

In our study, we did not acquire turbulence intensity directly from experiment results. Therefore, we focused on the turbulent mixing length as a factor related to the sediment mobility in debris flows to consider the turbulence intensity. It is influenced by kinetic energy dissipation due to the interstitial fluid turbulence in debris flow. Referring to a previous study (Egashira et al., 1986), we defined the turbulent mixing length l as follows:

$$l = \sqrt{k_f} \left(\frac{1 - C_{solid}}{C_{solid}} \right)^{\frac{1}{3}} d \quad (8)$$

where k_f is the coefficient, $\sqrt{k_f} = 0.5$ from previous studies, and d is for the diameter of the sediment particles behaving as solid phase.

Fig. 5a shows the l/d , ratio of turbulent mixing length and sediment diameter on the horizontal axis. The vertical axis shows ρ/ρ_w , a non-dimensional parameter calculated by dividing fluid phase density ρ by the density of pure water ρ_w . In the graph, the plots show the supplied sediment concentration and supplied sediment discharge. From the results, when l/d becomes large, ρ/ρ_w also becomes large. When the supplied sediment concentration C is high, l/d becomes small and ρ/ρ_w becomes large. Regarding the different supplied sediment concentrations C , the inclination of the relationship between l/d and ρ/ρ_w becomes steep when C is high. Calculating l/d from equation (8), it is assumed that when the sediment concentration C becomes higher, l/d becomes smaller and turbulence is less likely to occur. However, in our study, when sediment concentration C became higher, l/d became lower, but showing larger ρ/ρ_w and turbulence was more likely to occur.

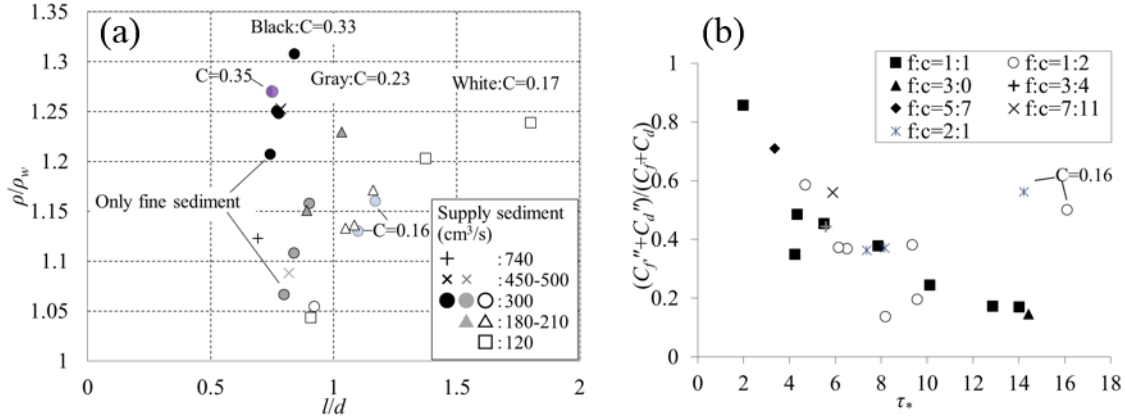


Fig. 5. Results (a) showing the relationship between the ratio of turbulent mixing length and diameter, and ρ/ρ_w , (b) showing the relationship between the dimensionless tractive force τ_* and ratio of sediment acting in fluid phase

With the same supplied sediment concentration C , cases with smaller supplied sediment discharge showed larger l/d and ρ/ρ_w , and cause a greater shift in the sediment phase to fluid phase. The previously noted trend was clear in Case 13, $C = 0.33$ and supplied sediment was 300 cm³/s; in Case 18, $C = 0.23$ and supplied sediment was 180 cm³/s; and in Case 15, $C = 0.17$ and supplied sediment was 120 cm³/s. With $C = 0.33$, Case 1 showed the smallest l/d and ρ/ρ_w , which was also the largest supplied sediment discharge case. This was an example to show that larger sediment discharge was presumed to inhibit turbulence and the phase shift. The second smallest l/d and ρ/ρ_w with $C = 0.33$ was Case 16 for which the supplied sediment was 300 cm³/s, case including only fine sediment. Except for Case 16, the next larger l/d and ρ/ρ_w with $C = 0.33$ was for supplied sediment of 500 cm³/s and then for 300 cm³/s. Therefore, this also matches the trend that smaller sediment discharge shows larger l/d and ρ/ρ_w and causes more phase shift. When $C = 0.23$, Case 4 had the smallest l/d and ρ/ρ_w , the supplied sediment discharge was 300 cm³/s, case including only fine sediment. Except for Case 4, Case 3 was the largest supplied sediment discharge with 450 cm³/s, showing the smallest l/d and ρ/ρ_w for $C = 0.23$. With $C = 0.17$, except for the smallest l/d and ρ/ρ_w in Case 17, the trend shows smaller supplied sediment discharge cases with larger l/d and ρ/ρ_w . In Fig. 5a, the supplied concentration of $C = 0.35$ is only one plot, but it matches the trend that when the concentration becomes large, l/d is lower and ρ/ρ_w is higher. For $C = 0.16$, two plots in Fig. 5a show trend similar to that for the $C = 0.17$ cases.

Next, we considered the indicator for turbulence intensity applying the dimensionless tractive force τ_* , which is widely used as a parameter for sediment movability on riverbeds given by the equation

$$\tau_* = \frac{\rho_w h \sin \theta}{(\sigma - \rho_w) d_f} \quad (9)$$

Fig. 5b shows the dimensionless tractive force τ_* on the horizontal axis. The vertical axis shows $(C_f + C_d)/(C_f + C_d)$, the ratio of sediment that behaves as fluid phase. From these results, when τ_* becomes large, the ratio of sediment behaving as fluid phase becomes small. This trend was different from those of recent studies using similar parameters u_*/w_0 for the indicator of sediment mobility, ratio of friction velocity u_* , and settling velocity w_0 . In a recent study (Nakatani et al., 2018), when u_*/w_0 became large, the ratio of sediment behaving as fluid phase became larger. The difference occurred because the supplied sediment discharge was fixed in the recent study. However, in the current

study, we applied several conditions of supplied sediment discharge. Therefore, with high sediment concentrations and also large supplied discharge conditions, it is assumed that river-bed shear force to which sediment particles are exposed while flowing, and the energy loss due to particle collision, become larger. This results in lower mobility, and in lower fluid density. In cases with smaller sediment concentration ($C = 0.16$), the two plots in Fig. 5b show rather large ratios compared with other cases with higher sediment concentrations.

4. Conclusions

In this study, we conducted hydraulic experiments with sediments of two different particle diameters, defined as fine sediment and coarse sediment. We applied equilibrium methods and also took into account the contribution of the sediment to the increase in the fluid phase density due to sediment phase shift to fluid phase. From the results, all the cases showed a shift of fine sediment to fluid phase. Furthermore, in some cases, not only fine sediments, but some part of the coarse sediments as well, indicated to behave as fluid phase. Sediment phase shift presumed to happen because of flow turbulence resulting from the factors sediment concentration, mixture of particles of different sizes, and the supplied sediment discharge. Higher total sediment concentration, and a higher proportion of coarse sediment (rather than only the fine particle content), indicated to increase the fluid phase density. Cases with smaller total sediment discharge showed higher fluid phase density in same concentration. In this study, we focused on turbulent mixing length as turbulence intensity, and found that higher sediment concentration cases showed smaller turbulent mixing length, but also showed higher fluid density. We also found that larger dimensionless tractive force linked to smaller ratios of particles behaving as fluid phase. This was opposite the trends in other recent studies. For future studies, we will aim to measure turbulence intensity from experiments to consider further mechanism of phase shift.

On the other hand, some studies claim that the sediment will not behave as either fluid or solid phase in debris flows (e.g. Sakai et al, 2016). We will consider it from different aspects such as applying resistance coefficients. In future work, we aim to propose a method for estimating the sediment phase shift to fluid phase, and apply these results in realistic debris flow simulations containing fine sediments, for more effective planning of countermeasure projects.

Acknowledgements

The study was supported by JSPS KAKENHI Grant No. 15K16312, Grant-in-Aid for Young Scientists (B). For the channel experiments, we used the facilities in the Ujigawa Hydraulics Laboratory of Disaster Prevention Research Institute, Kyoto University (Ujigawa Open Laboratory).

References

- Egashira, S., Ashida, K., Yajima, H. and Takahama, J., 1989, Constitutive equations of debris flow, Kyoto University Disaster Prevention Research Institute Annuals, v.32, B-2, p.487-499 (Japanese with English abstract).
- Hotta, N. and Miyamoto, K., 2008, Phase classification of laboratory debris flows over a rigid bed based on the relative flow depth and friction coefficients, International Journal of Erosion Control Engineering, v. 1, no. 2, p. 54-61.
- Iverson, R.M., 1997, The physics of debris flows, Reviews of Geophysics, AGU Publications, 35, p.245-296.
- Kaibori, M., Hasegawa, Y., Yamashita, Y., Nakatani, K., et al., 2018, Sediment related disaster due to heavy rainfall in Hiroshima Prefecture in July, Journal of the Japan Society of Erosion Control Engineering, v.71, no.4, p.49-60 (Japanese with English abstract).
- Ministry of Land, Infrastructure, Transport and Tourism, Water and Disaster Management Bureau, Sabo Division, 2014, Meeting Materials for Strengthening Countermeasures against Sediment Disasters, Subcommittee for structural countermeasures (in Japanese) http://www.mlit.go.jp/river/sabo/dosya_kyouka/140207_hard/140207_hard_shiry01.pdf (accessed Nov 2018).
- Nakatani, K., Furuya, T., Hasegawa, Y., Kosugi, K. and Satofuka, Y., 2018, Study on fine sediment phase change factors and influence on debris flow behavior, Journal of the Japan Society of Erosion Control Engineering, v.70, no.6, p.3-11 (Japanese with English abstract).
- Nishiguchi, Y., Uchida, T., Tamura, K. and Satofuka, Y., 2011, Prediction of run-out process for a debris flow triggered by a deep rapid landslide, Proceedings of 5th Debris Flow Hazard Mitigation Conference, p.477-485. doi: 10.4408/IJEGE.2011-03.B-053
- Sakai, Y., Hotta, N. Hasegawa, Y. and Nakatani, K., 2016, The model calculation of the velocity of steady-state debris flow containing finer sediment, Abstract EP21C-0887 presented at 2016 Fall Meeting, AGU, San Francisco, California, 12-16 December.
- Suzuki, T., Uchida, T. and Okamoto, A., 2013, Resolution of the discontinuity with the changes of sediment transport form in numerical simulation, Journal of the Japan Society of Erosion Control Engineering, v.66, no.2, p.21-30 (Japanese with English abstract).
- Takahashi, T., 1991, Debris Flow. Balkema, Rotterdam, 165p.
- Uchida, T., Nishiguchi, Y., Nakatani, K., Satofuka, Y., Yamakoshi, T., Okamoto, A. and Mizuyama, T., 2013, New Numerical Simulation Procedure for Large-scale Debris Flows (Kanao-LS), International Journal of Erosion Control Engineering v. 6, no. 2, p.58-67.
- Wada, T., Furuya, T., Nakatani, K., Satofuka, Y. and Mizuyama, T., 2015, Experimental study on the concentration of coarser particles at the frontal segment of a debris flow, International Journal of Erosion Control Engineering, v.8, no.2, p.20-30.